APPLICATION OF COMPUTER VISION TECHNIQUES TO SUPPORT IN THE RESTORATION OF HISTORICAL BUILDINGS

L. A. Ruiz *, J. L. Lerma , J. Gimeno

Dept. of Cartographic Engineering, Geodesy and Photogrammetry, Polytechnical University of Valencia, Cº de Vera s/n, 46022 Valencia (Spain)
laruiz@cgf.upv.es

KEY WORDS: Cultural Heritage, Classification, Texture, Camera (CCD), Cartography

ABSTRACT:

This paper describes the use of computer vision techniques to obtain cartography of materials and damages, in a semi-automatic way, of indoor façades of historical buildings, as a support to planify the restoration works. For this purpose, a cost-effective equipment is designed to acquire digital images from the visible and near infrared regions of the spectrum, and spectral and texture classification techniques are used to convert those images into informational classes. The equipment is composed of a monochromatic CCD camera, sensitive to the visible and NIR, with a peak of sensitivity at about 760 nm. The camera sends the signal to a frame grabber connected to a computer, where the image is processed. After calibration of the camera, 5 images centred at different spectral wavelengths (from 400 to 900 nm.) are acquired using optical filters. The scene is illuminated using diffuse light to avoid shadows on materials. Radiometric adjustment and geometrical registration are made, and then a mosaic of the images is composed using ground control points.
In addition to the spectral images, spatial information is obtained from textural features extracted by mean of the co-occurrence matrix, energy filters and multi-resolution analysis using a wavelet transform. A statistical selection process of the most relevant features is made, and the final classification is evaluated attending to the information provided by archaeologists and architects that carry out the restoration works. The methodology is applied indoors to a monument and the results are discussed, as well as some improvements that should be made in the future to integrate the equipment in order to be operative in the field.

1. INTRODUCTION

An important effort in the restoration of historical buildings is the generation of cartography of materials and damages of some façades before starting with the restoration works. The thematic maps of damages and pathologies are valuable tools for planning and are usually made manually by specialists in the interpretation of such damages and materials (archaeologists, architects,…). In this sense, there is an increasing interest to have this cartography of specific areas available in a digital form, and to be able to update it and compare it every time a new work is started in a monument. This would allow to integrate the information into a GIS, so the different technicians and experts could use it as a reference in the decision taking tasks for restoration of the cultural heritage.

There are examples of application of computer vision techniques based on CCD cameras to apply photogrammetric methods in order to extract measures from indoor façades, and getting quality digital pictures for the interpretation by experts and to catalogue specific parts of monuments (Hongo et al.). However, the use of pattern recognition techniques to identify materials and pathologies for the restoration tasks is an open area for researching. Lerma and Ruiz (1999, 2000) obtained spectral bands from a digital camera (visible) and an analogical camera with infrared film (NIR), and combined them with textural features to classify materials in outdoor façades. But the use of different types of cameras made difficult the combination of visible and NIR bands, as well as the integration of the equipment in the field.

The aims of this work were:

- The integration and testing of a computer vision system for the acquisition, in the field, of visible and NIR spectral information about materials of façades, with a lighting system to take indoor images.
- The development and evaluation of a combined spectral and textural classification process, based on the images acquired with that equipment and including preprocessing and mosaicking of the scenes, for the generation of cartography of specific materials as a support for the restoration tasks.

The selected site for the tests was a part of a wall in one of the chambers of the *Baths of El Almirante*, some middle-age baths located in Valencia (Spain), that have been experimenting a dynamic evolution along the years. There were almost no entrance of natural light. In addition, the state of degradation of the wall, with a diversity of layers of materials in a small area, made it appropriate for testing the equipment and the proposed methodology of classification.

2. MATERIALS AND METHODS

2.1 Equipment

The image acquisition system was composed of a Hitachi KP-F2A near-infrared progressive scan CCD camera, with a spectral response that extends from 400 to about 1000 nm, and a peak of sensitivity at 760 nm (figure 1). Zoom macro lens from 8 mm to 48 mm and four optical exchangeable filters were used, obtaining five spectral bands: blue, green, red+NIR (above 650nm), NIR (above 800nm), and the panchromatic band when no filter was used (figure 1). The output was a

standard RS-170 video signal. The CCD was connected to a Matrox Meteor-II frame grabber, capturing and digitising the images to 640 x 480 pixels and 8 bits/pixel. The data were transmitted via the PC-bus to the computer memory for processing.

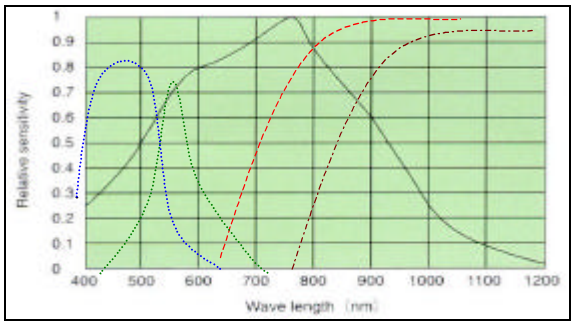

Figure 1. Spectral sensitivity response of the CCD (continuous) and transmission curves of the 4 spectral filters (dashed).

The illumination was provided by four portable halogen lamps with screens to diffuse the light and to avoid shadows and specular reflections.

2.2 Camera Calibration

Some experimental tests were conducted for geometric calibration of the camera, as reported by Lerma et al. (2002)., using sequences of 5 images with every type of filter and computing exterior and interior orientation parameters. The study shows that there is a high variability in the calibration parameters, so the geometrical reliability of these cameras is poor. However, in terms of spatial resolution, the accuracy needed for these non-photogrammetric applications can be achieved by adequating the lens and the distance to the object.

2.3 Data Acquisition and Preprocessing

Once the work site was selected and some preliminary tests made, the images were acquired using the equipment described above. The camera was fixed on a tripod and rotated on its vertical axis to take three overlapped images covering the part of the wall object of study. Due to the different angle of observation of the camera for each image, the illumination function should be corrected by means of radiometric adjustment, and the positional distortions by means of geometric correction before doing the final mosaic of the complete area.

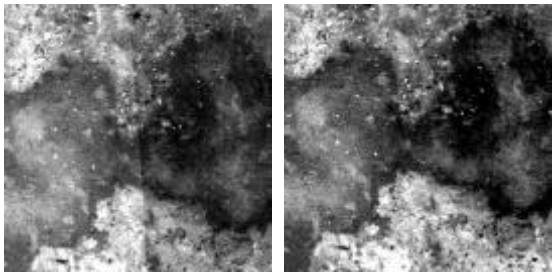

Figure . Detail of overlapping area between two images before (left) and after (right) the radiometric adjustment.

First, a geometric registration between the 5 spectral bands of each image was made, in order to correct the subtle camera movements made while exchanging the optical filters. Then, a geometric registration, using second order polynomial transformation based on control points taken on the overlapping areas, was made to obtain the initial mosaic of the three images.

The radiometric adjustment was made by matching the histogram of two of the images respect to the third one with a better contrast. This method is based upon the modification of the cumulative histogram of an image according to the cumulative histogram of the reference image. A detail of the overlapping area between two images, before and after the radiometric correction, is showed on figure 2. The final mosaic after applying the geometric and radiometric corrections is showed on figure 3.

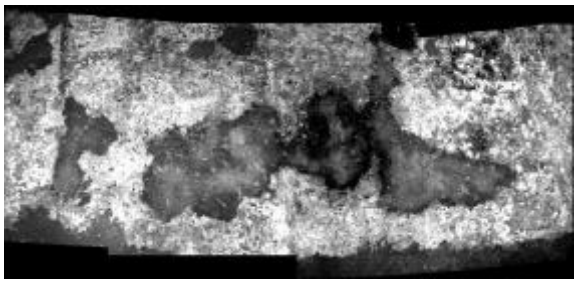

Figure 3. Mosaic after the geometric and radiometric corrections.

2.4 Feature extraction

Two main groups of features were used for classification: spectral and textural. The first group was composed by the 5 visible and NIR bands defined by the transmission properties of the filters and the spectral sensitivity of the CCD. The texture group was composed of 5 statistical features derived from the grey levels coocurrence matrix (GLCM), based on those proposed by Haralick (1973), and 6 features computed as the variance of a 21 x 21 neighbourhood from the images representing the details of a wavelet transform with three levels of decomposition. The process for feature extraction is showed in figure 4.

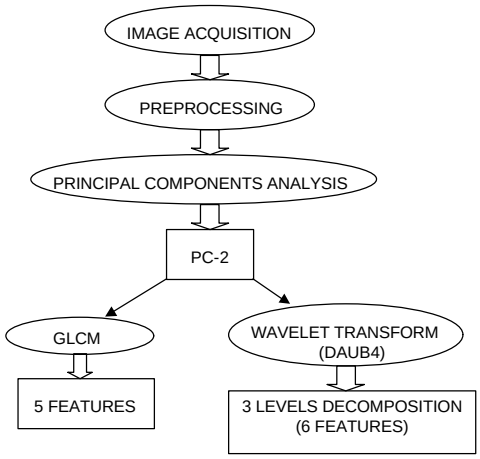

Figura 4. Process of texture feature extraction (*PC-2: 2nd principal component; GLCM: grey levels coocurrence matrix; DAUB4: Daubechies-4*).

A principal components analysis was performed over the 5 initial spectral variables. Since the second component revealed a better enhancement of the textures present, it was chosen as the base image for texture feature extraction.

The texture of an image deals with the spatial distribution and dependence among the grey levels in a local region. The elements of the GLCM, $P(i,j)$, represent the relative frequencies of two grey levels *i* and *j*, separated by a distance *d* along a given direction. The expression for the normalised coocurrence matrix is

$$p(i,j) = \frac{P(i,j)}{\sum_{i=0}^{N_g-1}\sum_{j=0}^{N_g-1} P(i,j)}$$

where N_g represents the number of grey levels available. We used a distance of one pixel and, since there was not directionality in our texture classes, take the average of the four initial directions. After testing several window sizes, we finally used a 21 x 21 pixels neighbourhood. The 5 GLCM features computed are specified in table 1.

Feature	Expression
Uniformity	$\sum_{i=0}^{N_g-1}\sum_{j=0}^{N_g-1} p(i,j)^2$
Contrast	$\sum_{i=0}^{N_g-1}\sum_{j=0}^{N_g-1} (i-j)^2 \cdot p(i,j)$
Mean (*)	$m = \sum_{i=0}^{N_g-1} i \cdot p_x(i)$
Variance	$\sum_{i=0}^{N_g-1}\sum_{j=0}^{N_g-1} (i-m)^2 \cdot p(i,j)$
Product Moment	$\sum_{i=0}^{N_g-1}\sum_{j=0}^{N_g-1} (i-m)\cdot(j-m)\cdot p(i,j)$

(*) $p_x(i) = \sum_{j=0}^{N_g-1} p(i,j)$

Table 1. GLCM texture features used.

A wavelet is a scaled and translated version of an elemental function called *mother wavelet*

$$y_{s,u}(x) = \frac{1}{\sqrt{s}} y\left(\frac{x-u}{s}\right) \qquad u \in \Re \qquad s \in \Re^+$$

where *s* is the scale parameter and *u* the translation parameter. The wavelet decomposition of a function can be computed by applying each of these wavelets to the function itself

$$Wf(s,u) = \int_{\Re} f(x) \frac{1}{\sqrt{s}} y^*\left(\frac{x-u}{s}\right) dx$$

In practice, the extension to the 2-D discrete case is usually performed by means of a product of 1-D low pass and high pass filters (Walker, 1999). The original image is thus decomposed into a set of subimages at several scales, some of them contain the *averages* of the original image at a particular scale, and others represent the *details*. Since most relevant texture information has been removed by iteratively low pass filtering, the *average images* are not usually considered to obtain the texture features (Van de Wouver, 1999). Therefore, they were computed from the *detail images*, applying three levels of decomposition and using the wavelet *Daubechies 4*. For each of the three levels, the sums of the details, before and after applying the inverse transform were computed, generating 6 new images. Then, the 6 final wavelet texture features used in the application were obtained as the statistical variance of the 21 x 21 neighbourhood around each pixel (Figure 5).

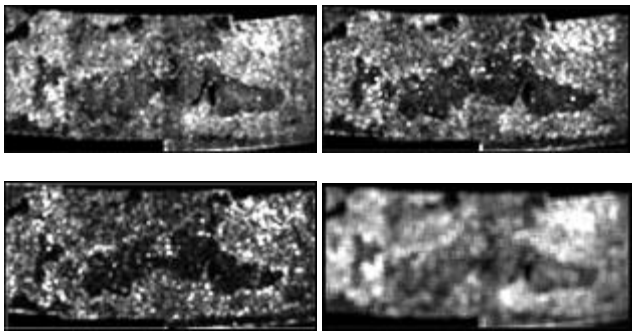

Figure 5. Four texture features computed from the *detail* images of the wavelet (*Daubechies 4*) decomposition applied over the second principal component.

2.5 Classification

Once the 16 spectral and texture variables were computed, the classification process started with the definition of the classes that were useful for restoration. In this case, the materials to be characterized were: two types of *coating* with different moisture content; three layers of *lime* added in different times; and *dirty areas*. Initially, a class of *mortar* was introduced but after the separability analysis it was rejected. Figure 6 shows image examples of each material.

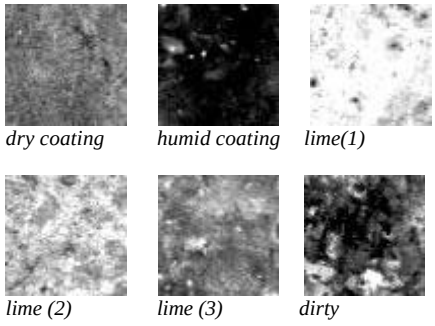

Figure 6. Examples of materials to classify.

A statistical separability analysis was performed to determine the window size that optimise our classification problem, to select the more reliable features and to define the final classes. This analysis was based on the average and minimum Jeffries-Matusita distances between classes In this step, the class *mortar* was rejected because of the poor results obtained.

After selecting representative samples for every class, the maximum likelihood supervised classification algorithm was applied. Finally, the evaluation of the process was based on the error matrix, computing the overall, producer and user accuracies. The two last accuracies give us information about the omission and commission errors, respectively. This provided analytical results about the comparative performance

of classification using different sets of variables: spectral, textural, and a combination of both.

3. RESULTS AND DISCUSSION

Table 2 and figure 7 show the performance of the classifications, in terms of overall accuracy, producer and user accuracies using different sets of variables: *spectral*, *texture* (coocurrence measures, wavelet features and both combined), and *spectral and textural* combined. The testing and learning samples used were the same, so the results are expected to be higher than the actual performance. Also, the texture results have been evaluated only inside the regions, not along the border areas where texture classification always introduce more errors. However, the results are valid for our comparison purposes.

SPECTRAL	***TEXTURE***			***SPEC+TEXT***
Visible+NIR	GLCM	Wavelets	GLCM+Wav.	All
74.9	82.9	58.1	92.2	95.3

Table 2. Overall accuracy results of the classifications using different sets of features.

Without considering the borders between classes, the texture classification performs better that the spectral, but the best results are achieved using a combination of spectral and texture variables (95.3%). Comparing only the texture features, the coocurrence measures are more efficient than the wavelet features, but this efficiency increases sharply when both set of features are included. One of the characteristics of the texture variables is their high correlation. It seems that these two set of variables (coocurrence and wavelets) contain complementary information to classify materials on facades. Something similar occurs when spectral and texture variables are combined.

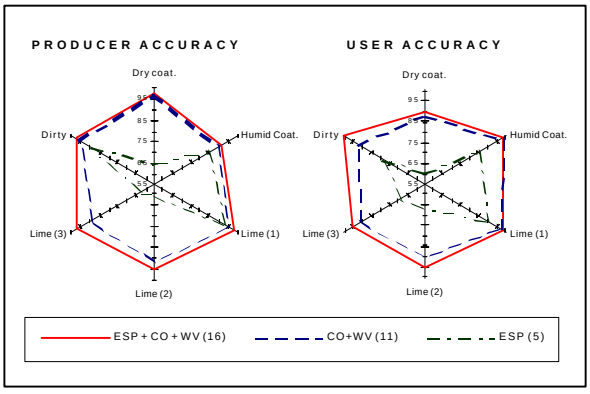

Figure 7. producer and user accuracies for the classification of 6 types of materials using three different sets of features: spectral (ESP), texture coocurrence and wavelets features (CO+WV), and all combined (ESP+CO+WV).

On the other hand, the principal components transformation and the selection of one component, in this case de second, allows to combine the texture information contained on all the visible and infrared spectral bands, but employing only one band for computing the texture features.

Finally, the figure 8 represents the image classified using the combination of all variables (spectral, coocurrence and wavelet features). Comparing it to the original mosaic of figure 3, it is noticeable the high level of coherence achieved, which is desirable for this type of applications.

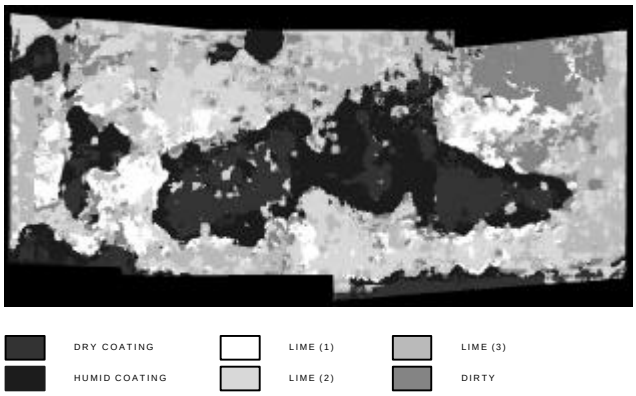

Figure 8. Classification of materials using all the features described.

4. CONCLUSIONS

The integration of a computer system based on a CCD camera and the use of filters to obtain multispectral information seems to be useful to cartography materials and damages on facades, but its portability, illumination capabilities and radiometric balance during acquisition need to be improved to be used in the heterogeneous field conditions.

A combination of spectral, and coocurrence and wavelet texture features provides encouraging results for classification of certain materials using this equipment.

REFERENCES

Haralick, R.M., K Shanmugam and Dinstein (1973). *Texture features for image classification*. IEEE Transactions on Systems, Man. and Cibernetics. SMC-3 : 610-622.

Hongo, K., Matsuoka, R., Fujiwara, S., Masuda, K., Aoki, S. (2000). *Development of Image-based Information System for Restoration of Cultural Heritage*. Intl. Arc. of Photogrammetry and Remote Sensing. XIX ISPRS Congress, pp 372-379.

Lerma, J.L., Ruiz, L.A. (1999). *Analysis of Historic Building Facades by Spectral and Texture Image Methods*. Proceedings of the VIII Spanish Symposium of Pattern Recognition and Image Analysis. Bilbao.

Lerma, J.L., Ruiz, L.A., Buchon, F. (2000). *Application of Spectral and Textural Classifications to Recognize Materials and Damages on Historic Building Facades.* International Archives of Photogrammetry and Remote Sensing. XIX ISPRS Congress, pp 480-483.

Lerma, J.L., Ruiz, L.A., Buchón, F., Pons, R., Galíndez, M. (2002). *Geometric Calibration of a Visible-NIR Video Camera*. Proceedings of the ISPRS Commission-V Symposium: Close-Range Imaging, Long-Range Vision. Corfu, Greece (in press).

Van de Vower, G., Scheunders, P., Van Dyck, D. (1999). *Statistical Texture Characterization from Discrete Wavelet Representations*. IEEE Trans. on Image Process. , Vol. 8 No. 4.

Walker, J.S. (1999). *A Primer on Wavelets and their Scientific Applications*. Chapman & Hall/CRC.

ACKNOWLEDGEMENTS

The authors would like to thank the Generalitat Valenciana for the financial support provided in the frame of the research project GV00-091-6.